Science of Sintering, **52** (2020) 87-95

doi:https://doi.org/10.2298/SOS2001087M

UDK: 546.57; 664.165; 546.264

Antimicrobial Effects of Carbonaceous Material Functionalized With Silver

Srđan Milanović, Nebojša Potkonjak, Vesna Mandušić, Đuro Čokeša, Jelena Hranisavljević, Branka Kaluđerović[*)]

Vinča Institute of Nuclear Sciences, University of Belgrade, P.O.Box 522, 11001 Belgrade, Serbia

Abstract:

Carbonaceous materials as well as its form functionalized with metallic silver have been prepared by hydrothermal carbonization of fructose. Results are presented to show that nanostructured silver was obtained through the functionalization process. The carbonaceous materials were characterized by: nitrogen adsorption/desorption measurement, XRD, SEM/EDS and FTIR. Samples functionalized with silver were analyzed by: XRD and SEM/EDS. The XRD analysis showed that the carbonaceous materials functionalized with silver by hydrothermal carbonization process were successfully performed. Size of silver particles was found to be approximately 32 nm, indicating formation of nanostructure. All samples were tested as an antimicrobial agent for water disinfection. Presence of nanostructured silver in the sample containing 1 mg/mL carbonaceous materials significantly decreased the number of CFU (dCFU = 97.33 %) if compared to the same sample containing the same amount of carbonaceous materials but without of silver (dCFU 65.33 %).

Keywords*: Carbonaceous material; Hydrothermal carbonization; Fructose; Silver nanoparticles; Antimicrobial effects.*

1. Introduction

The wide range of nanostructured carbon materials properties provides an attractive opportunity for various applications: environmental protection, energy-storage and conversion, in catalysis, for sensors and actuators, etc. Due to their biocompatibility there are various applications in medicine and pharmaceutical industry. [1-4].

Focus of the hydrothermal carbonization process (HTC) is production of nanostructured and functional carbonaceous materials. Major advance of this process could be found possibility of using cheap precursors such as saccharides or biomass, applying a simple one-step low cost synthesis process [5-11]. Due to the presence of a more reactive furanose unit, fructose has been found to dehydrate at lower temperature if compared with glucose [6, 7].

Medical applications of activated carbons are based on their powerful adsorption capacity unrivalled by any other material [12]. Silver is another element which is used for centuries in the treatment of burns, wounds and skin infections. Due to its bactericidal and bacteriostatic activity silver and its compounds are commonly used as an antimicrobial agents in various products such as antibacterial sprays, detergents, respirators, toothpastes, skin care products, etc. [13-16]. Beside its antimicrobial action, the effect of silver nanoparticles are

[*)] **Corresponding author:** branka@vin.bg.ac.rs

also investigated for it good characteristics toward the porosity decrease and the density increase, as well enhanced the hardness and fracture toughens of the Silver matrix composites [17, 18].

Global water resources are being rapidly exploited through unprecedented population growth resulting in water pollution [19]. Water laced with biological toxins and hazardous heavy metals and metalloids. Biological toxins are produced by bacteria, viruses, protozoa and fungi (mycotoxins). Water pollution is the leading worldwide cause of death and disease, e.g. due to water-borne diseases. The greatest water-borne threat to human health is bacterial contamination of drinking water sources, leading to outbreaks of diseases such as giardiasis, cholera, cryptosporidiosis, gastroenteritis, etc. [20].

In this study, carbonaceous materials as well as carbonaceous material functionalized with nanostructured silver have been prepared by the hydrothermal carbonization process and used to examine their antimicrobial activity.

2. Materials and Experimental Procedures

Fructose was used as a raw material for preparation of carbonaceous material. Fructose was diluted by 50 mL of phosphoric acid solution (pH = 0.65) and homogenized by magnetic stirrer. Than the solution was put in an autoclave and closed. After hydrothermal carbonization, at the 260 ^{o}C for 20 h, precipitate was collected by filtration and then washed repeatedly with distilled water and ethanol. Another sample was prepared in the same manner but in the reaction solution was added $AgNO_3$ to obtained 6mmol/L solution.

The investigated samples were characterized by, nitrogen adsorption/desorption isotherms, FTIR, XRD and SEM/EDS analysis.

Adsorption and desorption isotherms of nitrogen were measured on the carbonaceous samples at −196 °C using the gravimetric method by McBain balance. The specific surface area, S_{BET}, was calculated using Brunauer–Emmett–Teller (BET) theory [21]. Total pore volume, $V_{TOT,}$ was calculated using Gurwitch rule [21]. Pore size distribution was estimated by applying Horwath Kawazoe (HK) method (for micropores up to 1.5 nm) and Barrett, Joyner, and Halenda (BJH) method to the desorption branch of the isotherms [22, 23]. The external surface area, S_{EXT}, the total surface area, S_{TOT}, and the micropore volume, V_{mic}, of samples were estimated by using the high-resolution α_s plot method, from which the micropore surface can be also calculated by subtracting S_{EXT} from S_{TOT} [24, 25].

Spectroscopic studies of the synthesized materials were carried out in the mid infrared (MIR) regions (4000-400 cm^{-1}) using Fourier transforms infrared (FTIR) spectroscopy in transmission mode (Spectrum Two FT-IR spectrometer, Perkin Elmer) using pressed KBr pellet technique.

The X-ray diffraction (XRD) patterns were recorded by using the Ultima IV Rigaku diffractometer, equipped with CuKα radiation, using a generator voltage 40.0 kV and a generator current 40.0 mA. The range of 2θ between 10 and 90° was used in a continuous scan mode with a scanning step size of 0.02°.

The morphology and chemical composition of samples were identified using a JEOL JSM-6610LV Scanning Electron Microscope with an X-Max Energy Dispersive Spectrometer. Samples were coated with gold using a BALTEC-SCD-005 sputter coating device.

The assessment of antimicrobial effect is carried out in nutritious substrate - LB agar prepared with examined carbonaceous materials. Samples of water were collected during the winter season from brooklet located at the Vinca Institute and plated in Petri dishes containing LB-agar substrate. The volume of water samples (50 μL) were transferred on 8 cm Petri dish. Samples were collected in triplicate for each examined carbonaceous material. Upon incubation at 37 °C for 36 h in microbiological incubator, the number of CFUs (colony

forming units) was counted by using the Open CFU software. Plates are photographed after 48 h. The numbers of CFU represent the number of microorganisms (without identification) in the initial volume of water sample. Final results were expressed as % of decrease in number of visible colonies on LB-agar plates with addition of carbonaceous materials with/without silver nanoparticles compared with the control plate (only LB-agar). In both cases concentrations of carbonaceous materials were 1 mg/mL or 3 mg/mL.

3. Results and Discussion

The amount of nitrogen adsorption on the obtained carbonaceous sample is expressed by using comparison high resolution α_s plot (see Fig. 1). Sing et al. proposed α_s method in order to determine the micropore volume, V_{mic} and the external surface area, $S_{EXT,}$ which cannot be done by BET method [26]. The compares the obtained adsorption data with a standard isotherm of nitrogen adsorption on some non-porous solid. The reference data of nonporous carbon black were used as a standard for active carbon materials [24, 25].

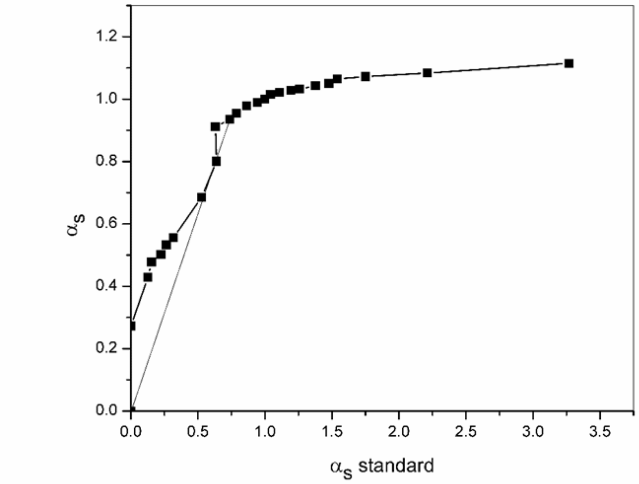

Fig. 1. High resolution α_s plot for carbonaceous material.

The α_s plot has two upward swings from the linearity below downward bending due to saturated filling at the higher α_s, region, as shown in Fig. 1. Existence of two upward swings in the α_s plot represents the characteristic of microporous carbon material [24, 25]. The upward swing ($\alpha_s < 0.3$) originates from enhanced adsorption by the micropores, while the other upward swing corresponds to the capillary condensation in mesopores. The calculated values also confirm this. Total specific surface area S_{TOT} is found to be S_{TOT} = 734 m^2/g. On the other hand the specific surface area calculated by BET method is S_{BET} = 893 m^2/g. If compared the results obtained from these two methods, it can be seen that the S_{TOT} is smaller than S_{BET} by 18 %. External surface area S_{EXT} calculated from Fig. 1 is 21 m^2/g, while micropore volume, V_{mic} is 0.413 cm^3/g. The total pore volume V_{TOT} is 0.451 cm^3/g. Results obtained suggest that S_{EXT} (the area of mezo and macro pores) represents only 2.9 % of S_{TOT}. This is in agreement with the percentage part of the mesopores volume (2.7 %) calculated from ration of V_{TOT} - V_{mic} and V_{TOT}. Obtained results suggest that investigated carbonaceous material has microporous structure [24, 25].

Microporous structure of the obtained carbonaceous material was also confirmed by pore size calculation. The pore size distribution is shown in Fig. 2. Pore size calculations were

based on slit shape pore geometry assumption. Pore size calculations were performed by HK method for micropores lower than 1.5 nm.

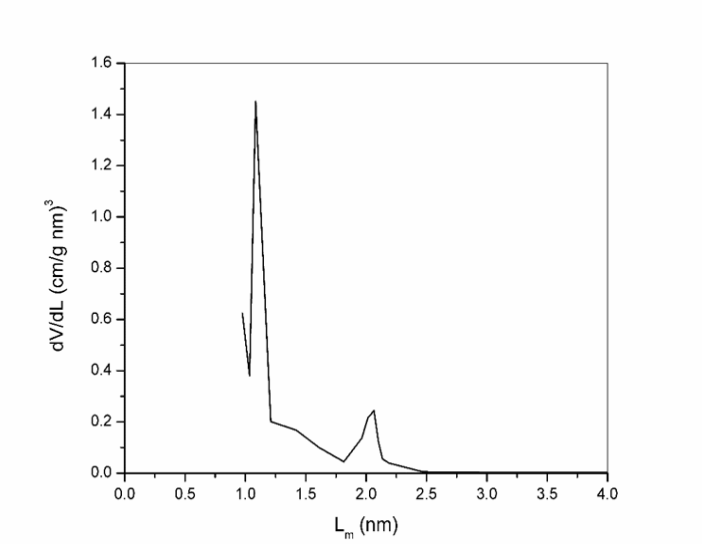

Fig. 2. Pore size distribution of the carbonaceous material.

This is due to the fact that accuracy of the method decreases for micropores size larger than 1.5 nm. In the case when pore size is larger than 1.5 nm pore size calculations were done using Kelvin's equation which founds the basis of the BJH method [21]. Generally, desorption isotherm data is more appropriate for pore size calculation than the adsorption isotherm data. It was observed from that the pore sizes ≈ 1.2 nm are dominantly present in the samples, Fig. 2.

Fig. 3 shows FTIR spectra of the obtained carbonaceous material. A broad band with a maximum at about 3406 cm^{-1} can be observed. This band can be assigned to the O–H stretching mode of hydroxyl groups and adsorbed water.

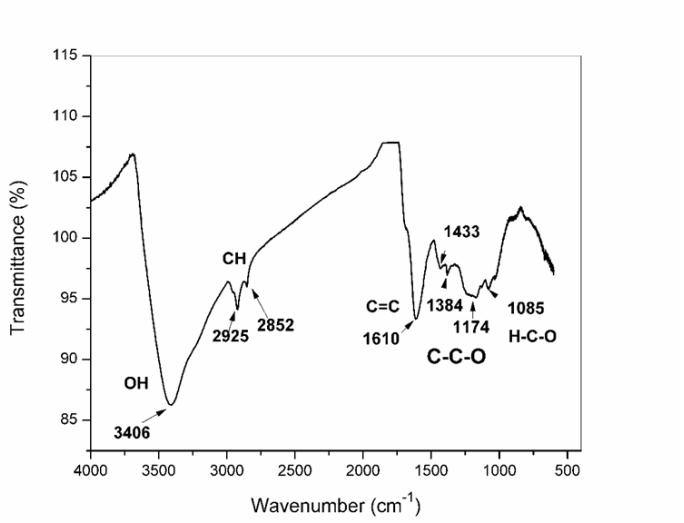

Fig. 3. FTIR analysis of the carbonaceous material.

The position and asymmetry of this band at lower wavenumbers indicate the presence of strong hydrogen bonds [27]. The bands at 2925 cm^{-1} and 2852 cm^{-1} can be assign to aliphatic C–H stretching in –CH_2–. The spectra also show a strong band at 1610 cm^{-1}

indicating the existence of C=C. The peaks at 1433 cm^{-1} and 1384 cm^{-1} are due $–CH_2–$ deformation and aromatic structure. Broad band's at 1300-1000 cm^{-1} have been assigned to C–O stretching in alcohols, phenols, ethers and esters [8, 27].

Structural characteristics of the functionalized samples are presented in Fig. 4 by the X-ray diffraction pattern of sample functionalized with Ag. The prominent peaks at 2Θ values of about 38°, 44°, 64°, 77° and 81° were indexed as (111), (200), (220), (311) and (222) Bragg's reflections, respectively [28]. The existence of these reflections are from crystal planes of face centered cubic (fcc) structure of silver. In order to estimate the crystalline domain size (d) Scherer diffraction formula was used.

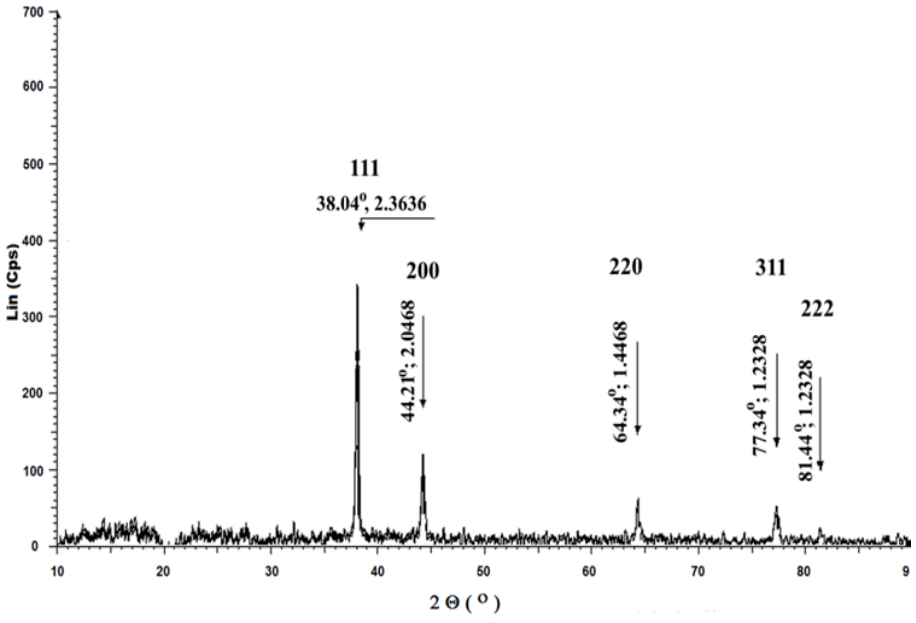

Fig. 4. XRD pattern of the carbonaceous material functionalized with silver.

The crystalline domain size was calculated using the data of most prominent peak i.e. from (111) reflection. The crystalline domain size of silver was found to be about 32 nm.

Morphology of the obtained carbonaceous materials without and with silver is presented by SEM micrographs, Fig. 5 (a) and (b), respectively.

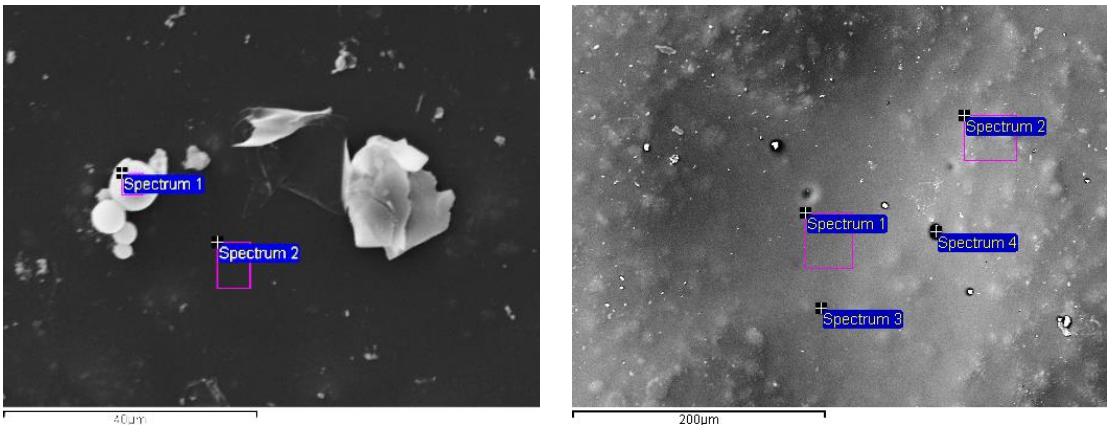

a) b)

Fig. 5. SEM micrographs of (a) carbonaceous sample, (b) sample with silver.

The hydrothermal reaction of fructose generates a solid residue, what is supposed to be formed by the merger of particles with a spherical morphology, shown in Fig. 5 (a). Some of these spherical particles have a diameter in the 2-8 μm range as evidenced by the SEM micrograph. After functionalization with silver, carbonaceous particles are poorly noticed. Silver particles cannot be seen at all on the SEM micrographs due to its size (32 nm), Fig. 5 (b).

Tab. I. EDS analysis of the carbonaceous sample (C) and sample functionalized with silver (Ag).

Spectrum	C/%	O/%	Ag/%
Spectrum C1	67.42	32.58	-
Spectrum C2	63.44	36.56	-
Spectrum Ag1	60.78	39.22	0.00
Spectrum Ag2	61.51	38.49	0.00
Spectrum Ag3	59.04	31.95	9.01
Spectrum Ag4	69.00	31.00	0.00

The results of EDS analysis of the carbonaceous sample from Fig. 5 (a) - Spectrums C and sample functionalized with silver from Fig. 5 (b) - Spectrums Ag are presented in Table I. The fact that silver was detected in only one from four spectrums (Spectrum Ag3) suggests that samples functionalized with silver are inhomogeneous. This could be explained by low concentration of $AgNO_3$ used in the sample preparation.

The EDS analysis of the carbonaceous material has demonstrated that the spherical particles in this sample has a similar carbon content as the rest of the material, Fig. 5 (a), Spectrums C1 and C2 in Table I. Furthermore, it was found that during the hydrothermal carbonization process mean value of carbon content increases from starting 40 % up to 65.43 %. This increase was found to be insignificantly lower for the samples functionalized with silver, see Spectrums Ag in Table I. Mean value of oxygen content was found to decrease from 53.33 % in started material to 34.57 % content in carbonaceous material.

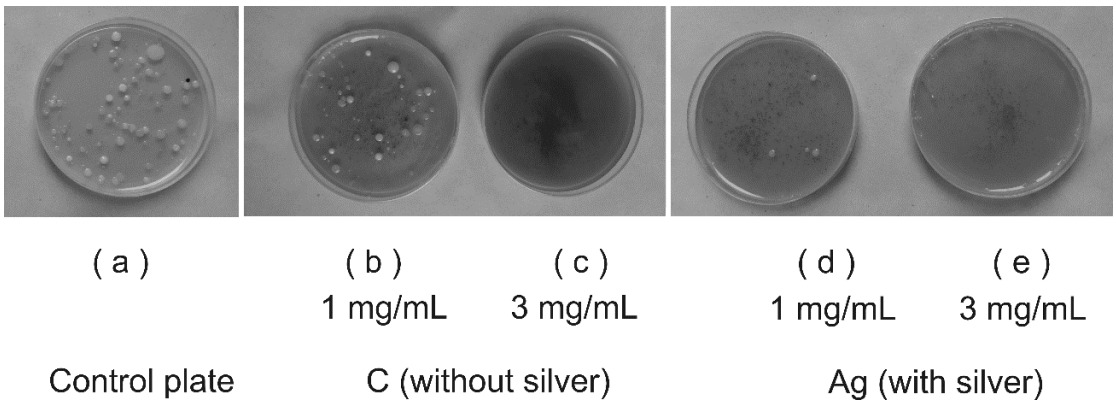

Fig. 6. CFU numbers: (a) LB agar control plate; LB agar plate with: (b) C 1 mg/mL; (c) C 3 mg/mL; (d) Ag 1mg/mL and (e) Ag 3 mg/mL.

The number of microbial colonies grown on LB agar plates are shown in Fig. 6 and results are summarized in Table II.

The number of CFU in control LB agar plate was 150 units, Fig. 6 (a). Decreases in the number of colony forming units (dCFU), expressed as percentage of CFU in control plate were as follow:

i) at the concentration of 1 mg/mL of carbonaceous material the decrease is significantly higher for samples functionalized with silver (97.33 %), Fig. 6 (d), Table II, than for carbonaceous samples (65,33%), Fig. 6 (b), Table II,

ii) at the concentration of 3 mg/mL, the complete inhibition of bacterial growth (100%) was achieved with both carbonaceous materials (without/with silver), Fig. 6 (c) and (e), Table II.

Tab. II. Influence of the type and the concentration of samples on the decrease of CFU (presented as dCFU / %).

Sample	**CFU**	**dCFU/%**	**CFU**	**dCFU/%**
Concentration	1 mg/mL	1 mg/mL	3 mg/mL	3 mg/mL
C	52	65.33	0	100
Ag	4	97.33	0	100

4. Conclusion

Formation of a solid microporous carbonaceous material was done under the hydrothermal conditions by the chemical activation of fructose with the phosphoric acid. Calculated according to Gurwitch rule, the total pores volume was 0.451 cm^3/g, while the micropores volume was 0.413 cm^3/g. It was found that carbonaceous material contains microsized spheres ranging from 2 μm to 8 μm in diameter. The diameter of these microspheres can be modulated by modifying of the synthesis conditions. Functionalization of this material with silver using the same hydrothermal carbonization process yielded the nanostructured silver (the crystalline domain size is 32 nm), embedded in microporous carbonaceous sample.

All the tested samples with or without nanostructured silver showed antimicrobial activity. Presence of nanostructured silver in the sample containing 1 mg/mL carbonaceous materials significantly decreased the number of CFU (dCFU = 97.33 %) if compared to the same sample containing the same amount of carbonaceous materials but without of silver (dCFU 65.33 %). With increase of the carbonaceous material concentration of in the substrate up to 3 mg/mL, antimicrobial effect of 100% was achieved with both materials.

Acknowledgments

The work has been supported by the Ministry of Education, Science and Technological Development of the Republic of Serbia under national projects No. III45005, 173049 and 172015.

5. References

1. K. Sattler, Carbon Nanomaterials Sourcebook, Vol. I and II Taylor & Francis, Boca Raton, USA, 2016.
2. T. J. Bandosz, M. J. Biggs, K. E. Gubbins, Y., Hattori, T. Iiyama, K. Kaneko, J. Pikunic, K.T. Thomson, in Chemistry and Physics of Carbon, L.R. Radovic Ed., Marcel Dekker Inc, New York, USA, 2003, 28, 41-228.

3. L. R. Radovic, in Carbon Materials for Electrochemical Energy Storage Systems: Advanced Materials and Technologies, F. Béguin and E. Frackowiak, Eds., CRC Press, Taylor&Francis, Boca Raton, USA, 2010, 163-219.
4. B. V. Kaludjerović, V. M. Jovanović, S.I. Stevanović, Ž. D. Bogdanov, Ultrason. Sonochem., 21 (2014) 782.
5. J. Ryu, Y.–W. Suh, D. J. Suh, D.J. Ahn, Carbon, 48 (2010) 1990.
6. C. Yao, Y. Shin, L-Q. Wang, C. F. Windisch, Jr., W.D. Samuels, B.W. Arey, C. Wang, W.M. Risen, Jr., G. J. Exarhos, J. Phys. Chem. C**,** 111 (2007) 15141.
7. X. Sun, Y. Li, Angew. Chem. Int. Ed., 43 (2004) 597.
8. M. Sevilla, A.B. Fuertes, Carbon, 47 (2009) 2281.
9. R. Demir-Cakan, N. Baccile, M. Antonietti, M. -M. Titirici, Chem. Mater., 21 (2009) 484.
10. B. Hu, K., Wang, L. Wu, S.-H. Yu, M. Antonietti, M.-M. Titirici, Adv. Mater., 22 (2010) 813.
11. S.S. Krstić, M.M. Kragović, V.M. Dodevski, A.D. Marinković, B.V. Kaluđerović, G. Žerjav, A. Pintar, M.C. Pagnacco, M.D. Stojmenović, Sci. Sintering, 50 (2018) 255.
12. S.V. Mikhalovsky, V.G. Nikolaev, in Activated Carbon Surfaces in Environmental Remediation. 1st ed.; Editor T.J. Bandosz, Elsevier Ltd. NY, USA, 2006, 529-561.
13. S. Prabhu. E. Poulose, Int. Nano Lett., 2 (2012) 32.
14. W.K. Jung, H.C. Koo, K.W. Kim, S. Shin, S.H. Kim, Y.H Park, Appl. Environ. Microbiol., 74 (2008) 2171.
15. M. Murphy, K. Ting, X. Zhang, C. Soo, Z. Zheng, J. Nanomater., 2015 (2015) 96918.
16. C. Marambio-Jones, E. M. V. Hoek, J. Nanopart. Res., 12 (2010) 1531.
17. N. Mansourirad, M. Ardestaniand, M. R. Afshar, Sci. Sintering, 50 (2018) 323.
18. M. Gabriela Téllez-Arias, José G. Miranda-Hernández, Oscar Olea-Mejía, J. Lemus-Ruiz, Eduardo Terrés, Sci. Sintering, 51 (2019) 175-187.
19. J. Eliasson, Nature, 517 (2015) 6.
20. Guidelines for drinking-water quality: fourth edition incorporating the first addendum. Geneva: World Health Organization; 2017. License: CC BY-NC-SA 3.0 IGO.
21. Y. Yhang, F. L.-Y. Lam, Z.-F. Yan, X. Hu, Chin. J. Chem. Phys., 19 (2006) 102.
22. G. Horvath, K. J. Kawazoe, Chem. Eng. Jpn., 16 (1983) 470.
23. E.P. Barrett, L.G. Joyner, P.P. Halend, J. Amer. Chem. Soc., 61 (1951) 373.
24. K. Kaneko, C. Ishii, M. Ruike, H. Kuwabara, Carbon, 30 (1992) 1075.
25. K. Kaneko, C. Ishii, H. Kanoh, Y. Hanzawa, N. Setoyama, T. Suzuki, Adv. Colloid Interface Sci., 76–77 (1998) 295.
26. K.S.W. Sing, Carbon, 27 (1998) 5.
27. J. Cveticanin, A. Krkljes, Z. Kacarevic-Popovic, M. Mitric, Z. Rakocevic, Dj. Trpkov, O. Neskovic, Appl. Surf. Sci., 256 (2010) 7048.
28. J. Zawadzki, in: P.A. Thrower, Editor, Chemistry and Physics of Carbon, New York: Marcel Dekker, USA, 1989, 21, 147-386.

Сажетак: *Карбонски материјали као и њихове функционализоване форме са метални сребром припремана су поступком хидротермалне карбонизација фруктозе. Резултати су показали да се приликом процеса функционализације добија наноструктурно сребро. Карбонски материјали су карактерисани следећим методама: мерењем адсорбције/десорбције азота, XRD, SEM/EDS и FTIR. Узорци функционализовани са сребром анализирани су помоћу: XRD и SEM/EDS метода. XRD анализа је показала да се процес хидротермалне карбонизације може успешно применити на функционализацију карбонског материјала са сребром. Нађено је да величина честица среба износи приближно 32 nm, што указује на формирање наноструктура. Сви узорци су тестирани као антимикробни агенси за дезинфекцију вода. Присуство наноструктурног сребра у узорку који је садржи 1 mg/mL карбонског*

материјала значајно смањује број CFU (dCFU = 97.33 %) ако се упореди са истим узорком који садржи исту количину карбонског материјала без сребра (dCFU 65.33 %).
***Кључне речи**: карбонски материјали, хидротермална карбонизација, фруктоза, наночестице сребра, антимикробни ефекат.*